Quaternary International 693 (2024) 38–48

Contents lists available at ScienceDirect

Quaternary International

journal homepage: www.elsevier.com/locate/quaint

Tree-ring stable isotopes in cellulose and lignin methoxy groups reveal different age-related behaviour

Anna Wieland [a,1,*], Philipp Römer [b,1,*], Max Torbenson [b], Markus Greule [a], Otmar Urban [c], Josef Čáslavský [c], Natálie Pernicová [c,d], Miroslav Trnka [c,d], Ulf Büntgen [c,e,f,g], Jan Esper [b,c], Frank Keppler [a,h]

[a] Institute of Earth Sciences, Heidelberg University, 69120, Heidelberg, Germany
[b] Department of Geography, Johannes Gutenberg University, 55099, Mainz, Germany
[c] Global Change Research Institute, Czech Academy of Sciences, 60300, Brno, Czech Republic
[d] Department of Agrosystems and Bioclimatology, Mendel University, 61300, Brno, Czech Republic
[e] Department of Geography, University of Cambridge, Cambridge, CB2 3EN, UK
[f] Department of Geography, Faculty of Science, Masaryk University, 61137, Brno, Czech Republic
[g] Swiss Federal Research Institute (WSL), 8903, Birmensdorf, Switzerland
[h] Heidelberg Center for the Environment (HCE), Heidelberg University, 69120, Heidelberg, Germany

ARTICLE INFO

Keywords:
Tree-ring stable isotopes
Cellulose
Lignin methoxy groups
Age trend
Pinus heldreichii
Northern Greece

ABSTRACT

Tree-ring stable isotopes (TRSI) have the unique ability to capture inter-annual to multi-millennial climate trends and extremes if the appropriate data and methods are combined. However, there is still an ongoing debate about age-related biases in TRSI measurements that potentially affect the fidelity of their chronologies and subsequent climate reconstructions.

Here, we investigate carbon and oxygen TRSI measurements in cellulose ($\delta^{13}C_{cell}$ and $\delta^{18}O_{cell}$) and carbon and hydrogen ratios in lignin methoxy groups ($\delta^{13}C_{meth}$ and $\delta^{2}H_{meth}$) of more than 60 living and relict pine (*Pinus heldreichii*) trees from northern Greece that span the period 512–2020 CE continuously. We identified significant ($p < 0.01$) level offsets between living and relict $\delta^{18}O_{cell}$ values (1.49 mUr) that preclude, among others, the combination of living and relict wood series for reliable age-trend assessment, and we found distinct differences between cellulose and methoxy TRSI chronologies including contrasting recent trends in carbon, oxygen, and hydrogen isotope ratios suggesting that varying environmental signals are retained in the TRSI proxies. Assessments are supported by comparisons with well-established ontogenetic trends in tree-ring width and latewood maximum density to identify significant ($p < 0.01$) age-trends in relict $\delta^{18}O_{cell}$ values between 50 and 190 years of cambial age, and in relict $\delta^{13}C_{meth}$ and $\delta^{2}H_{meth}$ values in tree rings older than 100 years. Relict $\delta^{13}C_{cell}$ values, on the other hand, show increasing values between 50 and 80 years of cambial age ($p < 0.01$), but no evidence for long-term trends beyond these early stages.

The combined assessment of multiple TRSI from cellulose and lignin methoxy groups contributes to a better understanding of the underlying physiological processes and extends the range of extractable climate information from the utilized tree-ring proxies. Our findings demonstrate that raw $\delta^{13}C_{cell}$ data from Mt. Smolikas can be used for climate calibration and reconstruction purposes without the need for standardization (expect for rings ≤80 years of cambial age), potentially providing new insights into long-term climate variability in the eastern Mediterranean region. $\delta^{18}O_{cell}$, $\delta^{13}C_{meth}$, and $\delta^{2}H_{meth}$ values, however, require detrending due to long-term age-related trends.

* Corresponding authors.
E-mail addresses: anna.wieland@geow.uni-heideberg.de (A. Wieland), phiroeme@uni-mainz.de (P. Römer).
[1] These authors contributed equally.

https://doi.org/10.1016/j.quaint.2024.02.004
Received 13 November 2023; Received in revised form 15 January 2024; Accepted 5 February 2024
Available online 19 February 2024

1. Introduction

Tree-ring stable isotope (TRSI) measurements of cellulose and lignin methoxy groups are important proxies for high-resolution paleoclimate reconstruction. While TRSI measurements of methoxy groups are relatively new compared to measurements of cellulose, both compounds are used to assess past climate information (e.g. Anhäuser et al., 2017; Büntgen et al., 2021; Esper et al., 2015; Hafner et al., 2011; Lu et al., 2022; Riechelmann et al., 2017; Treydte et al., 2001; Wieland et al., 2022). Combining proxies that have different controlling factors, such as growing-season temperatures or precipitation totals, increases the potential to reconstruct different seasonal climate variations at varying spatiotemporal scales from the same material (McCarroll et al., 2003; Mischel et al., 2015). Moreover, comparing various plant components provides additional information on differences in isotopic fractionation within variable biochemical pathways. To date, however, only two studies have compared the stable isotope ratios of cellulose and methoxy groups from the same material: Gori et al. (2013) and Mischel et al. (2015). Both studies compared the stable carbon ($\delta^{13}C$), oxygen ($\delta^{18}O$), and hydrogen ($\delta^{2}H$) TRSI values of whole wood, cellulose, and lignin methoxy groups and found that TRSI values of methoxy groups are influenced by different environmental and biochemical factors than those of cellulose and whole wood.

Classic tree-ring proxies such as tree-ring width (TRW) and maximum latewood density (MXD) need to be standardised prior to climate interpretation as both parameters include age-related trends (Bräker, 1981). However, removing age-related trends from a chronology induces a loss of low-frequency climate information (Cook et al., 1995). Several methods have been developed to preserve low-frequency variability (Briffa et al., 1992; Esper et al., 2003; Melvin and Briffa, 2008, 2014) but these techniques require large datasets that are typically composed of living and dead trees (Esper et al., 2004). Age-related trends can generally be divided into juvenile trends, including the first few decades of tree growth, and long-term trends throughout the trees' (varying) life spans. Juvenile effects have been documented in many TRSI chronologies (e.g. Duquesnay et al., 1998; Gagen et al., 2008, 2006; McCarroll and Loader, 2004; Raffalli-Delerce et al., 2004; Torbenson et al., 2022). To avoid biases from these trends, the first decades of tree rings can simply be omitted (Gagen et al., 2006). However, this is not applicable in the presence of long-term age-related trends (Helama et al., 2015). Esper et al. (2010) found age-related trends in cellulose TRSI chronologies, at a rate of −0.089 mUr decade^{-1} in $\delta^{18}O$ and +0.064 mUr decade^{-1} in $\delta^{13}C$ over the first 100 years of tree growth in *Pinus uncinata* trees in Spain. Similar values were later found in other studies with +0.035 mUr decade^{-1} in $\delta^{13}C$ values of pines from northern Scandinavia (Torbenson et al., 2022) and +0.04 mUr decade^{-1} in *Pinus sylvestris* L. from northern Finnish Lapland (Helama et al., 2015). However, there are also studies reporting no age trends in $\delta^{18}O$ and $\delta^{13}C$ values of oaks from the Czech Republic and in $\delta^{18}O$ values of pines from northern Scandinavia (Büntgen et al., 2020; Torbenson et al., 2022), suggesting that detrending is not necessary for paleoclimate reconstruction. Given the current state of knowledge, any isotopic dataset should therefore be tested for ontogenetic trends before using TRSI data for reconstruction purposes (Helama et al., 2015).

Discrepancies among studies could be related to species- and site-effects as well as methodological approaches including sample preparation, data pooling and truncation (Borella et al., 1999; Büntgen et al., 2020; Daux et al., 2018; Duffy et al., 2019; Leavitt, 2010; Loader et al., 2013; McCarroll and Loader, 2004). For reliable analysis of age trends, isotope data must contain a large number of samples with at least 10 individual series from different trees distributed over a range of centuries and thus growing under different climatic conditions. For $\delta^{13}C$ analysis, it is advantageous to use trees that grew prior to the strong atmospheric CO_2 changes during recent decades, as $\delta^{13}C$ values after 1850 CE must be corrected for the so-called Suess effect (decrease in atmospheric $\delta^{13}C_{CO2}$ values) (Keeling, 1979; McCarroll and Loader, 2004) and physiological responses due to increasing CO_2 concentrations (Keeling et al., 2017). These correction methods are still subject to large uncertainties, and the trend added by statistical corrections could cover potential age-related trends.

In this study, we present 62 individual $\delta^{18}O$ and $\delta^{13}C$ series of cellulose and 65 $\delta^{13}C$ and $\delta^{2}H$ series of methoxy groups from living and relict wood samples of *Pinus heldreichii* from Mt. Smolikas in northern Greece. The data are of annual and decadal resolution and developed from pines with different germination and end dates over the last 1500 years, making them well suited for assessing biological (non-climatic) age trends. However, significant ($p < 0.01$) level offsets between living and relict $\delta^{18}O$ and $\delta^{2}H$ values preclude the combination of living and relict wood series for reliable age-trend assessment. Therefore, to evaluate potential biological trends in TRSI, we used only the relict wood series, converted the TRSI series to a uniform decadal resolution since the methoxy-based relict wood samples were measured decadally, and compared the new TRSI data to the well-established TRW and MXD data from Mt. Smolikas (Esper et al., 2020a, 2021). Here, we (1) describe the key descriptive characteristics of the novel TRSI measurements, (2) quantify the observed differences between living and relict TRSI series, (3) assess the temporal persistence, stability, and magnitude of age-related trends in the relict TRSI data, and (4) infer important insights into chronology development for future paleoclimatic work.

2. Material and methods

2.1. Study site and tree-ring data

Between 2011 and 2020, 751 core and disc samples of *Pinus heldreichii* were collected at 2000–2100 m asl on Mt. Smolikas, Pindus Mountains in northwestern Greece (Fig. 1a) (40°05′N/20°55′E). Wood samples were processed according to standard dendrochronological techniques (Stokes and Smiley, 1996). TRW was measured using the high-precision Lintab (Rinntech GmbH, Heidelberg, Germany) and Velmex (Velmex Inc., Bloomfield, USA) devices, and MXD data was produced using a Walesch high precision DENDRO2003 X-ray densitometer (Walesch Electronic GmbH, Effretikon, Switzerland). Pith-offsets were estimated by visually matching the curvature of the innermost cross-dated rings with a set of concentric circles on a template (details in Klippel et al., 2017). TRSI measurements were performed on a representative subset of this wood collection, including well-preserved samples from living and relict trees. Stable carbon isotope measurements were produced on methoxy groups and cellulose ($\delta^{13}C_{meth}$ and $\delta^{13}C_{cell}$), whereas stable oxygen isotopes were only measured from cellulose ($\delta^{18}O_{cell}$) and stable hydrogen isotopes only from lignin methoxy groups ($\delta^{2}H_{meth}$) (Fig. 1c).

The TRSI data of methoxy (cellulose) include 65 (62) samples from the same 49 (46) relict and 16 living trees (Table 1). The individual TRSI series range from 512 to 2020 CE, with a constant sample replication ≥10 series from 841 to 2020 CE (Fig. 1b). Please note the stepwise distribution of uniformly aged TRSI samples with different start and end dates throughout the 1st and 2nd millennium CE.

Since isotopic measurements of methoxy groups prior to 1861 CE are decadal resolved, all other data sets including annually resolved TRW, MXD, $\delta^{13}C_{cell}$ and $\delta^{18}O_{cell}$ values were converted to the same resolution by averaging the annual values of each decade. Comparison of the annually resolved (only available for the cellulose TRSI over the entire chronology period) and decadal $\delta^{13}C_{cell}$ and $\delta^{18}O_{cell}$ mean chronologies support the accuracy of this averaging procedure for the assessment of long-term trends (Fig. S1). The triple TRSI data were compared with previously established TRW and MXD data from Mt. Smolikas (Esper et al., 2020a, 2021), which were truncated to meet the temporal length of the isotope series.

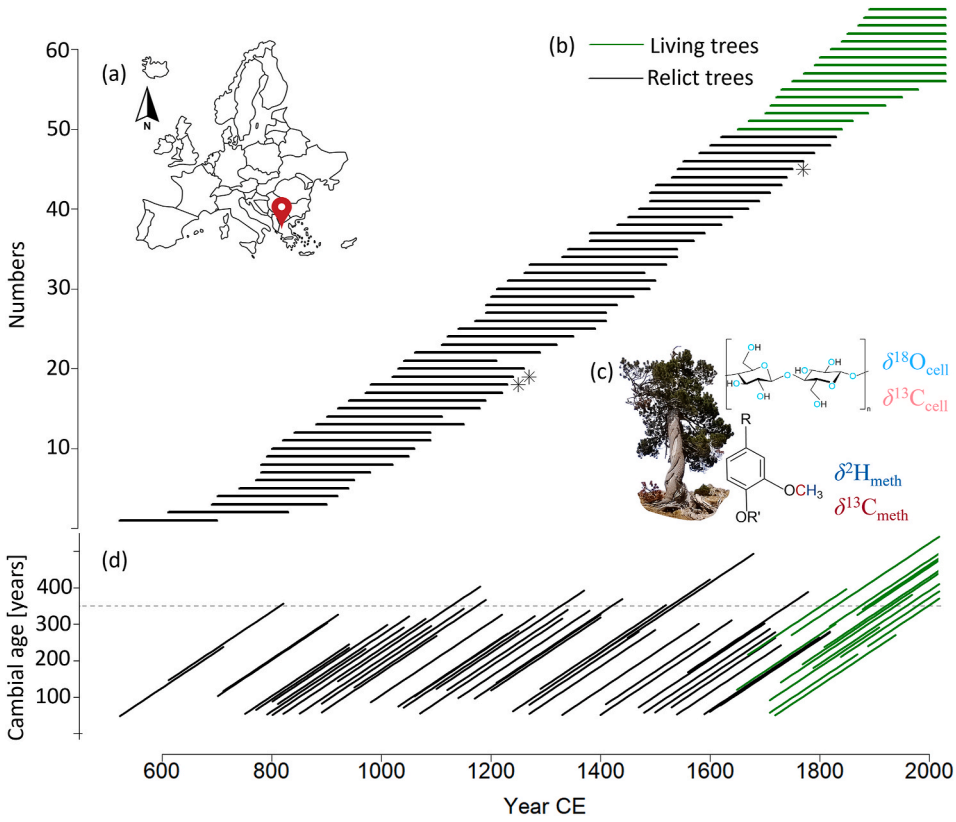

Fig. 1. Study site and proxy data. (a) Location of Mt. Smolikas in Europe. (b) Temporal distribution of the tree-ring stable isotope (TRSI) series. Asterisks denote series with only methoxy data. (c) *Pinus heldreichii* tree and schematic illustration of plant components used for TRSI measurement. (d) Cambial age of the individual tree-ring series.

Table 1
Proxy characteristics.

	TRW	MXD	$\delta^{13}C_{cell}$	$\delta^{13}C_{meth}$	$\delta^{18}O_{cell}$	$\delta^{2}H_{meth}$
No. series	751	192	62	65	62	65
No. living | relict trees	398 | 353	56 | 136	16 | 46	16 | 49	16 | 46	16 | 49
Mean segment length in years (SD)	320 (150)	294 (160)	224 (30)	220 (31)	224 (30)	220 (31)
Mean living | relict (SD)	0.76 (0.47) | 0.68 (0.45)	0.7 (0.05) | 0.68 (0.06)	−21.75 (0.68) | −21.43 (0.73)	−25.65 (1.14) | −25.77 (1.19)	33 (0.71) | 31.5 (1.51)	−259.12 (9.8) | −252.6 (9.9)

2.2. Stable isotope measurements

The modified Zeisel method (Greule et al., 2008, 2009; Keppler et al., 2004, 2007) was used for the determination of $\delta^{13}C_{meth}$ and $\delta^{2}H_{meth}$ values. For 5 mg ($\delta^{13}C$) or 7 mg ($\delta^{2}H$) grounded or sliced wood material, 250 µl hydroiodic acid was added, and based on the reaction between methyl ethers and esters and hydroiodic acid, iodomethane was formed (Zeisel, 1885). The samples were sealed with crimp caps in 1.5 ml crimp glass vials and heated for 30 min at 130 °C, followed by sample equilibration at room temperature. Afterwards, for $\delta^{13}C_{meth}$ ($\delta^{2}H_{meth}$) measurements, an aliquot of headspace between 10 and 90 µl was injected into a gas chromatograph – combustion (thermo conversion) – isotope ratio mass spectrometer (GC – C (TC) – IRMS) via an autosampler (A200S, CTC Analytics, Zwingen, Switzerland). For $\delta^{2}H_{meth}$ measurements an HP 6890N (Agilent, Santa Clara, USA) and for $\delta^{13}C_{meth}$ measurements a TraceGC (ThermoQuest Finnigan) was used. Both GCs were fitted with a DB – 5MS, Agilent J&W capillary column (length 30 m, internal diameter 0.25 mm, film thickness 0.5 µm).

For $\delta^{2}H_{meth}$ measurements, we used a 4:1 split injection and helium as carrier gas at a constant flow rate of 0.6 ml min^{-1}. A pyrolysis reactor (ceramic tube (Al_2O_3), length 320 mm, 0.5 mm i.d., reactor temperature 1450 °C) converted CH_3I to molecular hydrogen (H_2). For $\delta^{13}C_{meth}$ measurements a 20:1 split injection and helium as carrier gas at a constant flow rate of 1.8 ml min^{-1} was used. An oxidation reactor (ceramic tube (Al_2O_3), length 320 mm, internal diameter 0.5 mm) with Cu, Ni, and Pt wires inside (activated by oxygen) and a reaction temperature of 960 °C, oxidized CH_3I to CO_2. Stable isotopes in the resulting CO_2 and H_2 gases were transferred through a GC – Combustion III interface (ThermoQuest Finnigan) into the IRMS (Delta^{plus}XL, ThermoQuest Finnigan). The samples were normalized against two HUBG reference materials, respectively. For $\delta^{2}H_{meth}$ measurements HUBG 1 and 3 and for $\delta^{13}C_{meth}$ measurements HUBG 2 and 4 were used (Greule et al., 2019, 2020).

For the determination of $\delta^{18}O_{cell}$ and $\delta^{13}C_{cell}$ values the modified Jayme – Wise isolation method (Boettger et al., 2007) was used. About 0.5 mm wide shredded wood samples were packed into Teflon filter bags and washed twice for 2h at 60 °C with 5 % NaOH solution, followed by an additional wash with 7 % $NaClO_2$ solution for 30 h at 60 °C. To keep the pH between 4 and 5, acetic acid (99.8%) was added to the solution. Afterwards, the samples were dried at 50 °C for 24 h and locked in Eppendorf microtubes. For the stable isotope measurements, 0.5–1.0 mg of alpha-cellulose were placed into tin ($\delta^{13}C_{cell}$) and silver ($\delta^{18}O_{cell}$) capsules (Elementar Analysensysteme, Langenselbold, Germany). For $\delta^{18}O_{cell}$ determination the samples were pyrolyzed to CO_2 at 960 °C in oxygen and for $\delta^{13}C_{cell}$ analyses they were combusted to CO at 1450 °C in an inert atmosphere (helium) using an elemental analyzer varioPYRO cube (Elementar Analysensysteme, Germany). The resulting CO_2 and CO

gases were transferred by a continuous flow into the IRMS system (ISOPRIME 100, Manchester, UK). The stable isotope results were normalized using certified reference materials from the International Atomic Energy Agency (IAEA, Vienna, Austria) and United States Geological Survey (USGS, USA). $\delta^{13}C_{cell}$ values were referenced to caffeine (IAEA-600) and graphite (USGS24) and $\delta^{18}O_{cell}$ values to benzoic acids (IAEA-601 and IAEA-602).

Prior to the measurements, the IRMS systems were centered, tuned, and tested for precision (10 pulses of monitoring gas) and linearity (<0.4 mUr and <1 mUr/V ($\delta^{2}H_{meth}$), <0.02 mUr and <0.04 mUr/nA ($\delta^{18}O_{cell}$), 0.018 mUr and <0.06 mUr/V ($\delta^{13}C_{meth}$), <0.03 mUr and 0.04 mUr/nA ($\delta^{13}C_{cell}$)). For $\delta^{2}H_{meth}$ measurements, the H_3^+ factor was quantified prior to each set of isotopic measurements (<3.5 ppm/nA). The measurement accuracy was determined by analysing six (cellulose) or five (methoxy groups) consecutive samples. Average standard deviation was 0.042 mUr for $\delta^{13}C_{cell}$ (Römer et al., 2023), 0.089 mUr for $\delta^{18}O_{cell}$, between 0.01 and 0.25 mUr for $\delta^{13}C_{meth}$ (Greule et al., 2009) and 0.5 to 2 mUr for $\delta^{2}H_{meth}$ (Greule et al., 2008).

2.3. Data treatment

The delta (δ) notation is used for all TRSI values. It is important to note that the commonly used 'unit' per mil (‰) is not considered acceptable in the International System of Units (SI), as the SI discourages the use of a one-dimensional unit (Newell and Tiesinga, 2019) and ‰ is a 'quantity of dimension one', denoted by the symbol unit 1 in the SI (Brand and Coplen, 2012; Dybkaer, 2004). To address this issue and adhere to the principles of the SI, we use the term "Urey" (Ur, named after Urey (1948)) as the unit for expressing isotope delta values as suggested by Brand and Coplen (2012). Thus, 1 mUr is equivalent to 1 ‰. The $\delta^{18}O$, $\delta^{2}H$ and $\delta^{13}C$ values (mUr) were calculated as the deviation from the Vienna Standard Mean Ocean Water (VSMOW) ($\delta^{18}O$ and $\delta^{2}H$ values) and the Vienna Pee Dee Belemnite (VPDB) ($\delta^{13}C$ values).

$\delta^{13}C$ values after 1860 CE were corrected for the $\delta^{13}C_{CO2}$ decline in the atmosphere (Figs. 2–4), the so-called Suess effect (Keeling, 1979). Since this negative trend is a non-climatic, CO_2-driven effect, $\delta^{13}C$ values were corrected by adding the differences between $\delta^{13}C_{CO2}$ and the pre-industrial value (−6.41 mUr) to the measured $\delta^{13}C$ values for each year (McCarroll and Loader, 2004). Here, we used the $\delta^{13}C_{CO2}$ series from McCarroll and Loader (2004) and the Mauna Loa Observatory (Keeling et al., 2001; Mauna Loa Observatory, Hawaii, last access: 9 November 2023).

Coherences between the individual isotope series were assessed by calculating the mean inter-series correlation (Rbar) over the chronology period from 512 to 2020 CE using the R package dplR (Bunn, 2008).

2.4. Age trend analysis

An essential criterion for age trend assessments is an even distribution of tree rings over a wide range of calendar years, including rings grown under different climate conditions. In our study, we present decadally resolved TRSI data from 512 to 2020 CE characterized by a gradual distribution of samples over this extensive time span. The datasets consist of 46 (cellulose) and 49 (methoxy) relict and 16 living wood samples. The TRSI series of relict wood start between 512 and 1611 CE, while for living wood the start dates range from 1641 to 1881 CE. Hence, the relict wood TRSI series span over 1000 years, while the living wood TRSI series cover the recent 350 years including the significant climate and air composition changes since the mid-19th century. The average pith offset (PO) of the relict series is 84 years, compared to 201 years for the living trees. This difference in average PO estimates indicates that the TRSI values of living trees represent distinct older trees. When generating age-aligned TRSI series, tree ages above 350 years are therefore predominantly represented by living wood samples (Fig. 1d), which are strongly influenced by recent trend changes. To additionally avoid the impact of the Suess effect and physiological response correction in the age-aligned $\delta^{13}C_{meth}$ and $\delta^{13}C_{cell}$ series, age trend analyses for these proxies have been conducted using the relict wood only. The age trend analysis in this study focuses primarily on long-term age-related trends over the tree's lifespan, rather than juvenile effects that typically occur in the first few decades of tree growth. Hence, the first 50 years of cambial age were omitted and with a sample replication of ≥10 series, the age range from 50 to 355 years is covered. Age trend analyses of cellulose based TRSI series start at cambial age of 54 years to meet this minimum sample replication criterion.

To classify age-related trends, the TRSI chronologies were compared with 353 TRW and 136 MXD relict series. Age trends in TRW, MXD, $\delta^{13}C_{meth}$, $\delta^{2}H_{meth}$, $\delta^{18}O_{cell}$, and $\delta^{13}C_{cell}$ were analysed using the raw tree-ring data. For an accurate comparison among the proxies, all series were

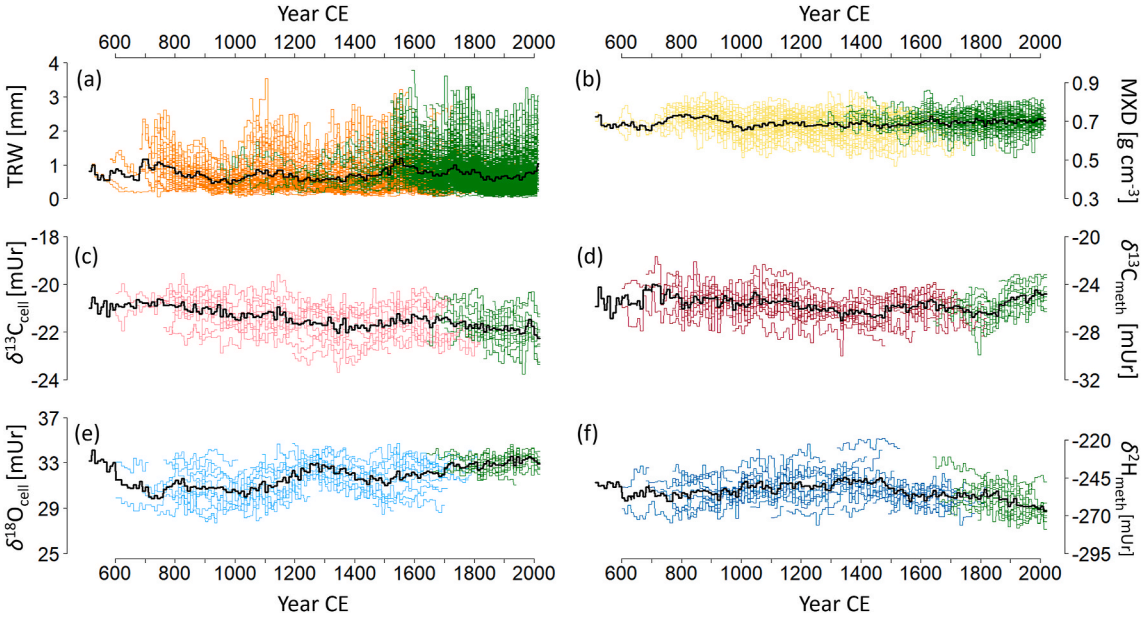

Fig. 2. Decadal resolved (a) TRW, (b) MXD, (c) $\delta^{13}C_{cell}$, (d) $\delta^{13}C_{meth}$, (e) $\delta^{18}O_{cell}$, and (f) $\delta^{2}H_{meth}$ series from 512 to 2020 CE. Green curves are measurements from living trees and coloured series from relict wood. Bold black curves are the mean chronologies.

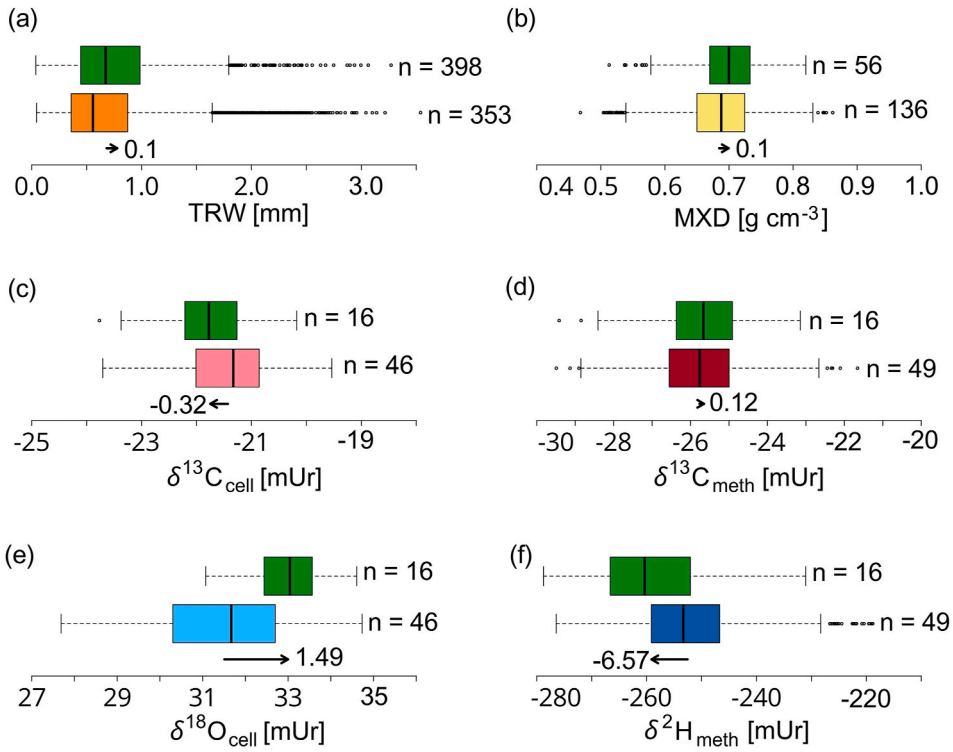

Fig. 3. Distribution and range of (a) TRW, (b) MXD, (c) $\delta^{13}C_{cell}$, (d) $\delta^{13}C_{meth}$, (e) $\delta^{18}O_{cell}$, and (f) $\delta^{2}H_{meth}$ values. Green boxes correspond to the living trees, while other colours represent the proxy-specific relict wood (same colour code as in Fig. 2). Vertical black lines represent the median (50th percentile), boxes represent the 25th and 75th percentiles, whiskers represent the 95% confidence interval, and points denote outliers. Numbers next to the arrows indicate the offset between the living and relict means ($\Delta_{liv/rel}$). Numbers next to the boxplots indicate sample replication.

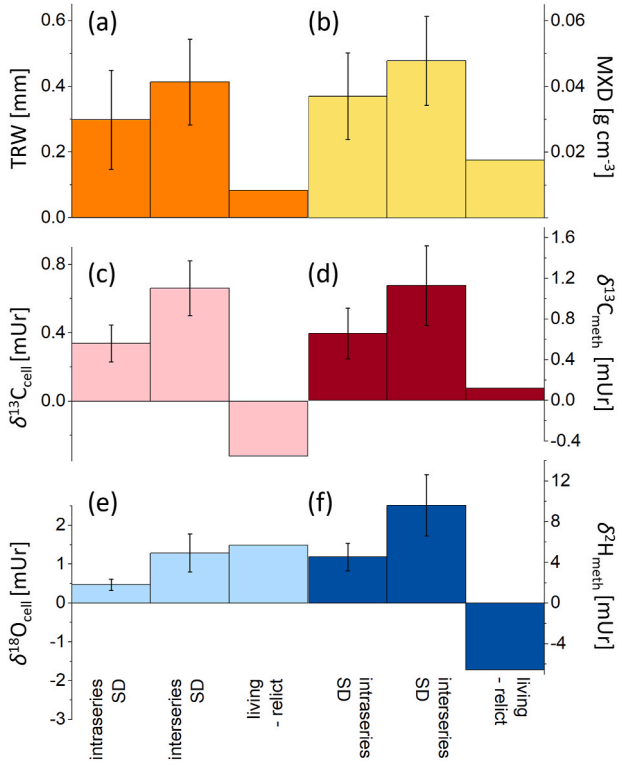

Fig. 4. Intra-series standard deviation (mean SD within the individual series), inter-series standard deviation (mean SD between all series in a certain decade) and mean offset between living and relict wood ($\Delta_{liv/rel}$) calculated for (a) TRW, (b) MXD, (c) $\delta^{13}C_{cell}$, (d) $\delta^{13}C_{meth}$, (e) $\delta^{18}O_{cell}$, and (f) $\delta^{2}H_{meth}$.

z-transformed before calculating mean chronologies. Individual series were aligned by their biological age considering the pith offset of each sample. Age trends were estimated using linear regression fitted to the raw age-aligned series (Fig. S2) and the arithmetic mean of the z-transformed series. This procedure was performed considering different time intervals. We started the regression windows with variable lengths, always beginning at tree age 50 (Fig. 6) or 100 (Fig. S6). The endpoint, on the other hand, initially began at tree age 70 or 170 and were subsequently shifted in 10-year intervals. Due to the calculation of z-scores, trends within individual series are preserved, but level offsets between the series are removed, leading to a potential underestimation of long-term trends across the series. To test whether this trend calculation is biased by the z-transformation, we additionally estimated age trends using TRSI anomalies derived from subtracting the mean of the common period 202–238 years from each series (Figs. S4 and S5). Significances of trends were calculated using the modified Mann-Kendall test (Hamed and Rao, 1998) adapted for autocorrelated datasets.

3. Results

3.1. Data characteristics

Mean Rbar values of annual $\delta^{13}C_{cell}$ and $\delta^{18}O_{cell}$ values are highly significant ($p < 0.001$) over the chronology period (512–2020 CE) with $r = 0.74$ and $r = 0.56$, respectively, pointing to a strong environmental forcing of the two cellulose-based isotope ratios. By transforming the data to decadal resolution, however, mean Rbar values decrease to 0.43 ($\delta^{13}C_{cell}$) and 0.44 ($\delta^{18}O_{cell}$) ($p < 0.05$). The Rbar values of $\delta^{13}C_{cell}$ and $\delta^{18}O_{cell}$ values calculated from 512 to 2020 CE are higher than those of decadal resolved $\delta^{13}C_{meth}$ and $\delta^{2}H_{meth}$ values with $r = 0.25$ and $r = 0.34$ (Table 2).

The $\delta^{13}C_{cell}$ and $\delta^{13}C_{meth}$ values show a constantly decreasing trend between 512 and 1860 CE, followed by an increasing trend in $\delta^{13}C_{meth}$

Table 2
Proxy covariance and age-trend estimates.

	Raw data					
	TRW [mm]	**MXD [g cm^{-3}]**	**$\delta^{13}C_{cell}$ [mUr]**	**$\delta^{13}C_{meth}$ [mUr]**	**$\delta^{18}O_{cell}$ [mUr]**	**$\delta^{2}H_{meth}$ [mUr]**
Rbar annual (p-value)	0.55 (<0.001)	0.55 (<0.001)	0.74 (<0.001)	–	0.56 (<0.001)	–
Rbar decadal (p-value)	0.43 (0.03)	0.27 (0.13)	0.43 (0.04)	0.25 (0.2)	0.44 (0.04)	0.34 (0.11)
Trend decade^{-1} (1820–2020)	+0.0012	$+3.68 \times 10^{-5}$	−0.00086	+0.0097	+0.003	−0.055
	Age-aligned normalized data					
	TRW [mm decade^{-1}]	**MXD [g cm^{-3}decade^{-1}]**	**$\delta^{13}C_{cell}$ [mUr decade^{-1}]**	**$\delta^{13}C_{meth}$ [mUr decade^{-1}]**	**$\delta^{18}O_{cell}$ [mUr decade^{-1}]**	**$\delta^{2}H_{meth}$ [mUr decade^{-1}]**
Age trend (50–350 years)	−0.0042	−0.0021	−0.0009	−0.0022	−0.0005	+0.0031
Age trend (subset period)	−0.02 (50–70)	+0.012 (50–70)	+0.027 (50–80)	−0.003 (100–350)	−0.0074 (50–120)	+0.004 (100–350)

values and a decreasing trend in $\delta^{13}C_{cell}$ values thereafter (Fig. 2). The $\delta^{18}O_{cell}$ and $\delta^{2}H_{meth}$ values display more variability over time, as both proxies show an early decreasing trend until ~750 CE, followed by relatively stagnant values until ~1000 CE. After 1500 CE, $\delta^{18}O_{cell}$ values increase strongly at 0.004 mUr decade^{-1}, while $\delta^{2}H_{meth}$ values decrease steadily at −0.02 mUr decade^{-1}.

To assess the variability of the isotopic data and discern the influence of environmental changes or other factors, we calculated and compared the ranges of living and relict wood values for all six proxies (Fig. 3). While there are almost no differences between the living and relict wood of TRW, MXD, $\delta^{13}C_{cell}$, and $\delta^{13}C_{meth}$ ($\Delta_{liv/rel}$: mean difference between values of living and relict wood calculated across all series and calendar years), $\delta^{18}O_{cell}$ values of living wood are +1.49 mUr higher than the relict wood values. In contrast the living-tree $\delta^{2}H_{meth}$ values are −6.57 mUr lower than their relict wood counterparts (Fig. 3). Variance of living and relict wood is similarly in TRW, MXD, $\delta^{13}C_{cell}$, $\delta^{13}C_{meth}$, and $\delta^{2}H_{meth}$, except for $\delta^{18}O_{cell}$ showing increased interquartile ranges in relict wood (2.4) compared to the living wood (1.1) (Figs. 2 and 3). Comparable level offsets in $\delta^{18}O_{cell}$ values between living and relict wood were also seen when considering the common period from 1641 to 1820 CE, whereas offsets in $\delta^{2}H_{meth}$ values are no longer visible (Fig. S3).

Fig. 4 shows the mean intra-series standard deviation (SD of individual series), the mean inter-series SD (SD among series in each decade) and the $\Delta_{liv/rel}$. Intra-series SD is smaller than the inter-series SD for all six proxies. The intra- and inter-series SD of the methoxy-based TRSI

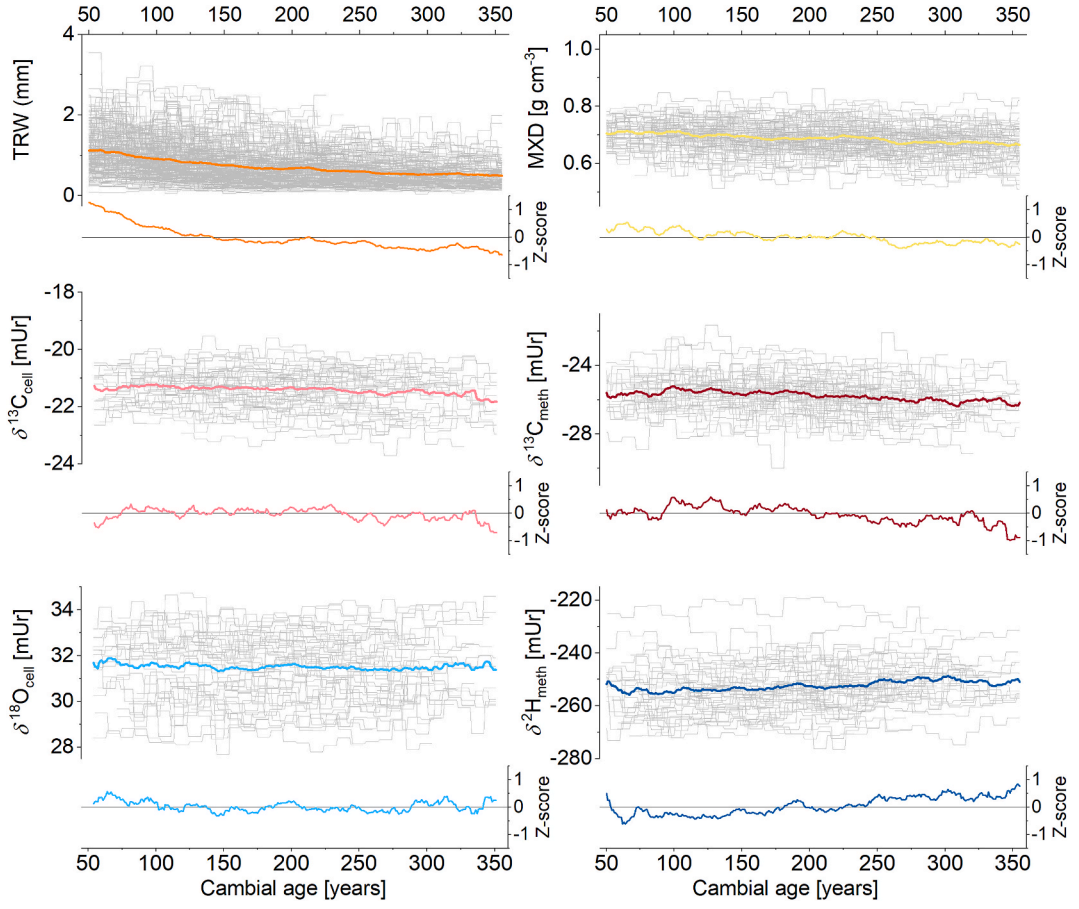

Fig. 5. Age-aligned TRW, MXD, $\delta^{13}C_{cell}$, $\delta^{13}C_{meth}$, $\delta^{18}O_{cell}$, and $\delta^{2}H_{meth}$ data of relict wood. Top curves in each panel show the raw series (grey) and their arithmetic means (coloured), lower curves are the means of the normalized data.

values is higher compared to the intra- and inter-series SD of the cellulose-derived TRSI values. Comparison between intra- and inter-series SD and $\Delta_{liv/rel}$ shows that $\Delta_{liv/rel}$ values in TRW, MXD, and $\delta^{13}C_{meth}$ are negligible compared to the intra- and inter-series SD. $\Delta_{liv/rel}$ in $\delta^{13}C_{cell}$ reaches similar amounts as the intra-series variation, indicating that the signal in the $\delta^{13}C_{cell}$ series is as high as the mean offset between living and relict wood values. $\Delta_{liv/rel}$ in $\delta^{18}O_{cell}$ and $\delta^{2}H_{meth}$ values are even more pronounced, as the $\Delta_{liv/rel}$ of $\delta^{18}O_{cell}$ exceeds the intra- and inter-series SD, and the $\Delta_{liv/rel}$ of $\delta^{2}H_{meth}$ values were considerably higher than the intra-series SD.

3.2. Age trend observations

The age-aligned raw and z-transformed TRW and MXD series show clear ontogenetic trends (Fig. 5). Similar to an exponential curve the decline in TRW is more pronounced in early years compared to the later stages. As a result, the mean TRW in year 350 is less than half of that in year 50. In contrast, the MXD series show a slight increase between 50 and 70 years of cambial age, followed by a persistent negative trend thereafter. The $\delta^{13}C_{cell}$ series show an initial increasing trend between 50 and 80 years, whereas the $\delta^{18}O_{cell}$ series show a decreasing trend until a tree age of 190 years (Table 2). Thereafter, neither $\delta^{13}C_{cell}$ nor $\delta^{18}O_{cell}$ series show any trend. In contrast, the $\delta^{2}H_{meth}$ series show decreasing values between 50 and 70 years of cambial age, and the $\delta^{13}C_{meth}$ series show short-term increasing trends between the tree ages of 90 and 100 years. Both $\delta^{13}C_{meth}$ and $\delta^{2}H_{meth}$ series exhibit further trends, especially after the tree age of 200 years.

A detailed slope examination of the z-transformed data (Fig. 6) verifies the trend observations in the raw data. TRW shows a consistent and significant ($p < 0.01$) decreasing trend over the 50–350 years of cambial age at a rate of -0.004 mm decade^{-1} (Table 2). On the other hand, MXD shows an initial increasing trend between 50 and 70 years, but this trend reverses and becomes significantly ($p < 0.01$) negative after 50–120 years. The initial positive trend in $\delta^{13}C_{cell}$ ($p < 0.01$ up to 50–100 years) is related to comparatively low $\delta^{13}C$ values at young tree ages (50–80 years), as no significant trends are found after a tree age of 100 years (Fig. S6). The initial decreasing $\delta^{18}O_{cell}$ values are significant between 50 and 190 years ($p < 0.01$, maximum slope from 50 to 120 years at -0.007 mUr decade^{-1}). For $\delta^{13}C_{meth}$ values, an initially increasing trend is found from 50 to 120 to 50–140 years at $p < 0.01$. However, significant decreasing trends of -0.002 mUr decade^{-1} years are observed from 50 to 290 years. In $\delta^{2}H_{meth}$, initially decreasing values at -0.04 mUr decade^{-1} are recorded at young ages (between 50 and 70 years), followed by significant increasing values from 50 to 210 years ($p < 0.01$).

Trend analyses of the mean relative chronologies (Fig. S5) support these findings and reveal significant ($p > 0.01$) positive trends in $\delta^{13}C_{cell}$ values between 50 and 100 years, as well as significant negative trends in $\delta^{13}C_{meth}$ and significant positive trends in $\delta^{2}H_{meth}$ values over the last third and the second half of the age aligned data, respectively. However, trend analyses reveal significant slopes in $\delta^{13}C_{meth}$ and $\delta^{2}H_{meth}$ to start earlier from 50 to 270 years and from 50 to 200 years, respectively, compared to the assessments of the mean z-transformed series. These differences, as well as the observed varying initial trends in $\delta^{18}O_{cell}$ and $\delta^{2}H_{meth}$ series are considered in the following discussion.

4. Discussion

4.1. Inter- and intra-proxy differences

The notable variations in stable carbon isotope values of cellulose, ranging from -22.2 to -20.9 mUr, and methoxy groups, ranging from -26.6 to -24.9 mUr, originate from different physiological processes that lead to considerable fractionation differences during the formation of the two plant components. While methoxy groups are depleted of ^{13}C by ~4 mUr compared to cellulose, the $\delta^{13}C$ values of cellulose and lignin vary within the same range with 1.3 mUr for $\delta^{13}C_{cell}$ values and 1.7 mUr for $\delta^{13}C_{meth}$ values. Therefore, by combining different plant components from the same trees, it is possible to gain a deeper insight into the varying biochemical formation processes. In addition, the combination of different climate proxies, deliberately chosen for their dissimilarity, offers the potential to increase the strength of the climate signal and the range of extractable climate information. The observed high Rbar between 512 and 2020 CE, especially in $\delta^{13}C_{cell}$ ($r = 0.74$) and $\delta^{18}O_{cell}$ ($r = 0.56$), are in line with previous observations from the Mediterranean region (Konter et al., 2014; Lukač et al., 2021; Römer et al., 2023) and support the importance of climate drivers on annual-to-decadal TRSI variability.

In this study we found discrepancies between the TRSI chronologies of cellulose and methoxy groups, particularly during the most recent

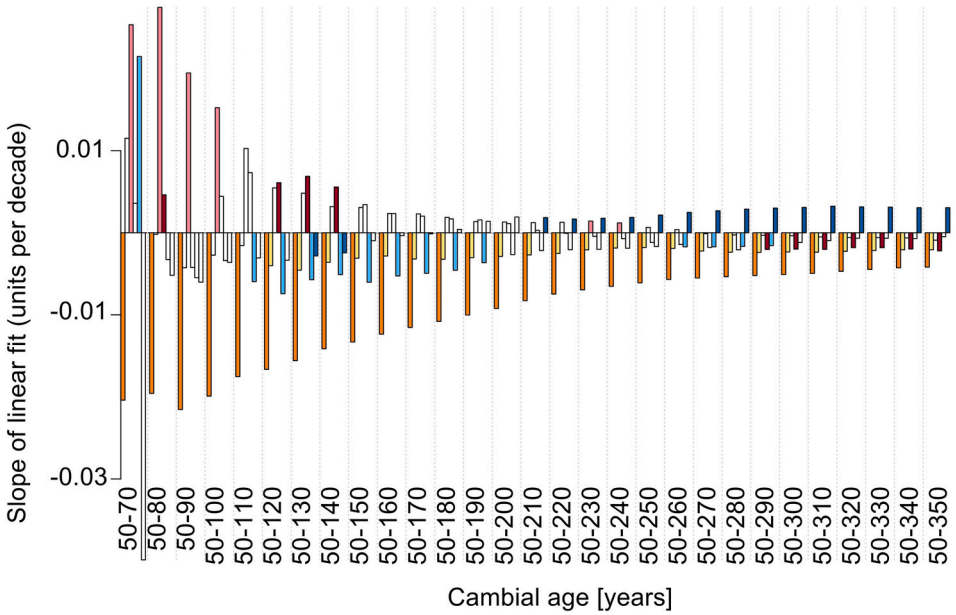

Fig. 6. Linear slopes of the mean z-transformed TRW (orange), MXD (yellow), $\delta^{13}C_{cell}$ (light red), $\delta^{13}C_{meth}$ (dark red), $\delta^{18}O_{cell}$ (light blue), and $\delta^{2}H_{meth}$ (dark blue) series. White bars represent non-significant ($p > 0.01$) and coloured bars significant slopes at $p < 0.01$.

200 years CE, where contrasting long-term trends in the carbon, oxygen, and hydrogen values of the two plant components are observed (Fig. 2, Table 2). Differences among TRSI data may be attributed to several factors. One plausible explanation is that the isotopic signature of the plant components is affected by varying environmental determinants, likely climatic factors such as temperature, drought, or precipitation. An alternative explanation is that the proxies may capture the same climate signal, but the seasonality of this signal varies due to temporal differences in the biosynthetic formation of these compounds. It is also possible that a mixture of factors collectively contributes to the observed variations. A previous study, comparing the isotopic composition of cellulose and lignin methoxy groups in *Pinus sylvestris* from central Germany, found that $\delta^{13}C_{cell}$ values are more sensitive to climatic variables of the entire growing season (from March to October), whereas $\delta^{13}C_{meth}$ values are more sensitive to climatic conditions at the beginning of the growing season (Mischel et al., 2015). Similar observations have been made for $\delta^{18}O_{cell}$ and $\delta^{2}H_{meth}$ values. While $\delta^{18}O_{cell}$ values were described to be primarily related to maximum air temperatures from March to October, $\delta^{2}H_{meth}$ values revealed significant ($p < 0.01$) correlations with maximum air temperatures from March to May (Mischel et al., 2015).

The observed offsets between living and relict $\delta^{2}H_{meth}$ values over the full chronology period (512–2020 CE) and the absence of similar offsets over the common period of the living and relict wood (1641–1820 CE, Fig. S3) show that $\Delta_{liv/rel}$ is mainly influenced by the strong negative trend inherent in the last 200 years of the chronology, which may reflect a significant change in environmental conditions.

In contrast, the $\Delta_{liv/rel}$ of the $\delta^{18}O_{cell}$ series seems to be influenced by a factor other than recent environmental change, as we find an offset between relict and living $\delta^{18}O_{cell}$ values over the entire chronology period as well as over the common period of living and relict wood. In addition to the isotopically lighter relict wood, strong level differences are observed in the relict wood series, with relict $\delta^{18}O_{cell}$ values covering a distinctly wider range than the living $\delta^{18}O_{cell}$ values (Figs. 2 and 3). The $\Delta_{liv/rel}$ of the $\delta^{18}O_{cell}$ data is of practical importance, as it exceeds the intra- and inter-series SD and is thus higher than the common isotope signal preserved in the chronology. The wider distribution of relict $\delta^{18}O_{cell}$ values could be related to cellulose decomposition associated with exchange processes with the surrounding water. Water exchange processes in $\delta^{18}O_{cell}$ but stable $\delta^{2}H_{meth}$ values could be explained by the fact that the lignin content in trees is more resistant to degradation than cellulose. Anhäuser et al. (2015) detailed losses of cellulose and lignin in foliar litter over a 27-month period for four different tree species. While three of the four species showed minor lignin losses up to 0.4 %, all species revealed large cellulose decreases ranging from 50.7 to 86.1 %. Although, the process of litter decomposition on a forest floor cannot be directly equated with the conditions observed at Mt. Smolikas, where climatic factors contribute to a slow rate of wood decomposition, the study by Anhäuser et al. (2015) shows that cellulose decomposition is accelerated compared to lignin decomposition.

A second and more likely factor for the high level differences in relict $\delta^{18}O_{cell}$ values is the influence of the sampled tree height. While living tree cores were always taken at breast height ~1.3 m above the ground, the disc samples of relict wood are from unknown tree heights due to centuries of decomposition (Fig. S7). Gaglioti et al. (2017) documented isotopically lighter $\delta^{18}O_{cell}$ values with increasing trunk height, and if the relict trees in this study are affected by a similar trend, the wood obtained in this study seems to represent mainly material from higher trunk heights. In addition to the negative $\Delta_{liv/rel}$ value, this would also explain the wider data distribution of the relict wood, as the series represent samples from diverse tree heights. Esper et al. (2020b) documented systematic changes of $\delta^{13}C_{cell}$ with stem height and sharply increasing values towards the tree crown. The $\delta^{13}C$ values in this study, however, do not appear to be affected by this tree-height bias, as none of the two $\delta^{13}C$ chronologies showed substantially high $\Delta_{liv/rel}$ values or strong differences in the data distribution of relict logs and living trees (Fig. 3). Possible explanations for stem-longitudinal $\delta^{13}C$ shifts include microclimatic changes and CO_2 stratification with tree height (Ehleringer et al., 1986; Esper et al., 2020b; Francey et al., 1985; Vogel, 1978). However, the trees used in this study grow in a rather open forest, and microclimatic differences and CO_2 stratification with tree height appear unlikely. Future studies should incorporate multiple stem-height measurements to assess this source of uncertainty.

4.2. Age trends in TRSI series

The gradual distribution of relict wood series and the multi-proxy approach of this study provide important insights into age-dependent trends in *Pinus heldreichii* from northern Greece. The trees used grew over several centuries from 512 to 1820 CE including warm and cold periods (Esper et al., 2020a), and climatic signals in the age-aligned series should therefore be levelled (Esper et al., 2003). Our results clearly demonstrate common age trends in traditional growth parameters (Bräker, 1981), including a decrease of −0.004 mm decade^{-1} in TRW and of −0.002 g cm^{-3} decade^{-1} in MXD between 50 and 350 years of cambial age.

Age-related trends are also apparent in all TRSI chronologies. We found initial short-term age-related trends in $\delta^{13}C_{cell}$ and $\delta^{2}H_{meth}$ values, decreasing trends in $\delta^{18}O_{cell}$ values until the tree age of 190 years, and significant negative and positive trends in $\delta^{13}C_{meth}$ and $\delta^{2}H_{meth}$ values from 50 to 290 and 50–210 years, respectively.

Most of the age trends in TRSI were of lesser magnitude than TRW and of shorter duration than MXD. While $\delta^{13}C_{cell}$ values clearly increase between 50 and 80 years of cambial age, no significant age-related trends are recorded thereafter. Compared to the age-trends in TRW, the juvenile $\delta^{13}C_{cell}$ trends are of comparable magnitude. Several $\delta^{13}C$ studies have documented this juvenile $\delta^{13}C$ trend during the first decades of cambial age (e.g. Esper et al., 2018, 2010; Francey and Farquhar, 1982; Konter et al., 2015; McCarroll and Pawellek, 2001; Torbenson et al., 2022; Treydte et al., 2001). The initially increasing $\delta^{13}C_{cell}$ values in this study could therefore be classified as a juvenile effect that appears to be extended (up to 80 years) in relation to the overall high tree ages of *Pinus heldreichii* at the Mt. Smolikas site (Konter et al., 2017). Common explanations for the juvenile effect in the early years of tree growth include shading of smaller trees and depleted CO_2 respiration from the forest floor (Francey and Farquhar, 1982; van der Merwe and Medina, 1991). These explanations, however, are unlikely to account for the juvenile trends in our $\delta^{13}C_{cell}$ series, as trees grow at high altitudes with a completely open canopy and almost permanent air mixing due to ever present wind. An alternative explanation refers to changes in hydraulic conductivity affecting stomatal conductance, which in turn affects carbon isotope values (McCarroll and Loader, 2004). With increasing tree height, soil to leaf hydraulic conductivity decreases, coupled with a steady reduction in stomatal conductance, which would lead to increasing $\delta^{13}C$ values until tree growth ceases (Esper et al., 2010; McDowell et al., 2002). Tree growth may not be completed after 80 years, but the observed increasing $\delta^{13}C_{cell}$ values may coincide with periods of greatest increasing height growth.

In contrast, $\delta^{2}H_{meth}$ values show an initial decreasing trend until a tree age of 70 years, from −251 to −255 mUr or −0.16 mUr decade^{-1} ($p < 0.01$, Fig. S5), followed by a smaller increasing trend starting at 100 years from −254 mUr to −251 mUr. Our study is the first to analyse long-term age-trends in TRSI of wood lignin methoxy groups, and there are no comparable methoxy-based results yet. Arosio et al. (2020) documented age-related trends in *Larix decidua* $\delta^{2}H_{cell}$ values with a decreasing trend in the first 50 years by ~7 mUr, followed by an increasing trend over the remaining tree ages up to 480 years by ~2.5 mUr. These findings are consistent with our observations. A possible explanation for the age-related trends in the juvenile phase could be that the shallow root systems of younger trees access different water sources than the deeply rooted older trees. In particular, soil water has often been characterized by an enrichment in ^{2}H from the deep to the shallow

soil layer due to evaporation processes and the loss of isotopically lighter water molecules (Allison et al., 1983; Lin and Sternberg, 1993). Our $\delta^{13}C_{meth}$ chronology shows a steep increase of $\delta^{13}C_{meth}$ values at a cambial age of ~100 years with constantly decreasing values thereafter, resulting in a long-term negative trend of −0.002 mUr decade^{-1} (50–350 years of cambial age, Fig. 6) and −0.003 mUr decade^{-1} (100–350 years of cambial age, Fig. S6). These trends are of comparable magnitude compared to the age-related trends in MXD (Fig. 6).

The $\delta^{18}O_{cell}$ values show a decreasing trend at the beginning, which is significant between 50 and 190 years of cambial age. This negative trend is not solely attributed to the relatively high $\delta^{18}O_{cell}$ values in younger tree ages (between 50 and 80 years), as significant ($p < 0.01$) negative trends are also observed when analysing cambial ages ranging from 100 to 170 and 100–180 years (Fig. S6). Changes in hydraulic conductivity with plant age could explain the juvenile trends in $\delta^{13}C_{cell}$ values, but not the decreasing trends in $\delta^{18}O_{cell}$ values, as reduced stomatal conductance would lead to higher $\delta^{18}O$ values (Barbour et al., 2004). But, similar to the initial negative trend in $\delta^{2}H_{meth}$ values, a change in the root system from shallower to deeper soils could also affect the $\delta^{18}O_{cell}$ values. Positive trends in $\delta^{2}H$ and negative trends in $\delta^{18}O$ of cellulose were also observed by Nakatsuka et al. (2020) and negative trends in $\delta^{18}O_{cell}$ were documented by Esper et al. (2010) and Treydte et al. (2006).

With the exception of the juvenile trends in $\delta^{13}C_{cell}$ and $\delta^{2}H_{meth}$ values, none of the observed long-term trends in TRSI are comparable to the age-related trends in TRW. However, the long-term trends in $\delta^{13}C_{meth}$ and $\delta^{2}H_{meth}$ are similar or even higher than the observed age trends in MXD (Fig. 6). Hence, juvenile effects in $\delta^{13}C_{cell}$ and $\delta^{2}H_{meth}$ should be considered when using the new Mt. Smolikas TRSI data for climate reconstruction. $\delta^{18}O_{cell}$, $\delta^{13}C_{meth}$, and $\delta^{2}H_{meth}$ chronologies must be detrended for proper climate signal determination, whereas no standardization is required for $\delta^{13}C_{cell}$ values. The current literature does not show a common pattern of long-term age-related trends in TRSI. While some studies found age-related trends during the juvenile period in $\delta^{13}C_{cell}$ values of pines (*Pinus cembra*) from the Swiss Alps (Arosio et al., 2020) and pines (*Pinus sylvestris*) from northern Finland (Gagen et al., 2008), others found age-related trends throughout the tree lifespans in pines (*Pinus uncinate*) from the Spanish Pyrenees (Esper et al., 2010) and in pines (*Pinus sylvestris*) from northern Scandinavia (Torbenson et al., 2022) and northern Lapland (Helama et al., 2015). However, there are also studies that found no evidence for age-related trends in oaks from the Czech Republic (Büntgen et al., 2020) and in larches from West Wales, UK (Kilroy et al., 2016). A similar inhomogeneous pattern can be observed for $\delta^{18}O_{cell}$ values, with significant age trends reported in pines (*Pinus uncinate*) from the Spanish Pyrenees (Esper et al., 2010) and the absence of such trends in pines (*Pinus sylvestris*) from northern Scandinavia (Torbenson et al., 2022) and in oaks from the Czech Republic (Büntgen et al., 2020) as well as after 100 years of cambial age in pines (*Pinus sylvestris*) from the Swiss Alps (Arosio et al., 2020). These contrasting observations could be related to the use of different tree species from different environments, but could also be due to different methodological approaches, such as measurements on different ring components (whole ring vs. latewood), pooling procedures or data pruning. Therefore, age dependencies must be tested in each isotopic dataset before TRSI measurements can be used for climate reconstructions.

5. Conclusion

In this study we analysed multi-isotope data from two different plant components, cellulose and lignin methoxy groups, to investigate biochemical fractionation differences and age-related trends. We compared stable carbon, oxygen, and hydrogen isotope ratios and found significant temporal variations between cellulose and methoxy groups, particularly over the past two centuries. Our findings suggest that different environmental factors control decadal variability and long-term trends of the two plant components.

While age dependencies in TRW and MXD are well-known and widely accepted in dendrochronological literature, the existence of age-related trends in TRSI is still strongly debated. Notably, no previous research has examined age dependencies in stable isotopes of methoxy groups. Our analysis of cellulose and methoxy TRSI series revealed initial increasing age trends in $\delta^{13}C_{cell}$ and initial decreasing trends in $\delta^{2}H_{meth}$ values, indicating the presence of an extended juvenile effect in both proxies. $\delta^{18}O_{cell}$ series show significant decreasing trends over the first 190 years of cambial age, whereas $\delta^{13}C_{meth}$ and $\delta^{2}H_{meth}$ series indicate decreasing and increasing trends starting at tree ages of 100 year. Hence, $\delta^{18}O_{cell}$, $\delta^{13}C_{meth}$, and $\delta^{2}H_{meth}$ series require detrending prior to climate reconstruction, whereas $\delta^{13}C_{cell}$ values may be used in paleoclimate analyses without detrending and therefore offer the unique potential to preserve low-frequency climate variability throughout the last two millennia CE. So far, the potential mechanisms behind age-related trends are not fully understood and the findings of this study highlight the complexity of ontogenetic trends in TRSI. It is therefore still important to test each site and tree species before using TRSI data for climate reconstructions.

Author contributions

A.W., P.R., F.K., and J.E. planned the study. A.W. and P.R. prepared the samples for isotope analyses. A.W. and M.G. measured the stable isotope ratios of lignin methoxy groups and J.Č., N.P., and O.U. measured the stable isotope ratios of cellulose. A.W. and P.R. drafted the manuscript with input from J.E., M.T., F.K., M.G., and U.B. All authors provided discussion and agreed to the final version of the manuscript.

Declaration of competing interest

The authors declare that they have no known competing financial interests or personal relationships that could have appeared to influence the work reported in this paper.

Acknowledgements

The authors thank Tilmann Büttner, Manuel Dienst, Yannik Esser, Christian Gnaneswaran, Nora Jubelius, Lisa Kinder, Lara Klippel, Markus Kochbeck, Paul Krusic, Inna Roshka, Luzie Schneider, Philipp Schulz, Marcel Wilhelm, and Birgit Wöste for field and laboratory work. This research has been supported by the German Research Foundation (Grand No. KE884/17-1 and ES161/12-1), the ERC Advanced Grant Monostar (AdG 882727), the Czech Science Foundation Grant HYDRO8 (No. 23-08049S), by the Internal Grant Agency of MENDELU (AF-IGA2022-IP-063), and the AdAgriF project (CZ.02.01.01/00/22_008/0004635).

Appendix A. Supplementary data

Supplementary data to this article can be found online at https://doi.org/10.1016/j.quaint.2024.02.004.

References

Allison, G., Barnes, C.J., Hughes, M.W., 1983. The distribution of deuterium and 18O in dry soils 2. Experientia (Basel) 64, 377–397. https://doi.org/10.1016/0022-1694(83)90078-1.

Anhäuser, T., Greule, M., Polag, D., Bowen, G.J., Keppler, F., 2017. Mean annual temperatures of mid-latitude regions derived from δ2H values of wood lignin methoxyl groups and its implications for paleoclimate studies. Sci. Total Environ. 574, 1276–1282. https://doi.org/10.1016/j.scitotenv.2016.07.189.

Anhäuser, T., Greule, M., Zech, M., Kalbitz, K., McRoberts, C., Keppler, F., 2015. Stable hydrogen and carbon isotope ratios of methoxyl groups during plant litter degradation. Isot. Environ. Health Stud. 51, 143–154. https://doi.org/10.1080/10256016.2015.1013540.

Arosio, T., Ziehmer, M.M., Nicolussi, K., Schlüchter, C., Leuenberger, M., 2020. Alpine Holocene tree-ring dataset: age-related trends in the stable isotopes of cellulose show

species-specific patterns. Biogeosciences 17, 4871–4882. https://doi.org/10.5194/bg-17-4871-2020.
Barbour, M.M., Roden, J.S., Farquhar, G.D., Ehleringer, J.R., 2004. Expressing leaf water and cellulose oxygen isotope ratios as enrichment above source water reveals evidence of a Péclet effect. Oecologia 138, 426–435. https://doi.org/10.1007/s00442-003-1449-3.
Boettger, T., Haupt, M., Kno, K., Weise, S.M., Waterhouse, J.S., Rinne, K.T., Loader, N.J., Sonninen, E., Jungner, H., Masson-delmotte, V., Stievenard, M., Pierre, M., Pazdur, A., Leuenberger, M., Filot, M., Saurer, M., Reynolds, C.E., Helle, G., Schleser, G.H., Ju, F., 2007. Wood cellulose preparation methods and mass spectrometric analyses of 13C, δ18O, and nonexchangeable δ2H values in cellulose, sugar, and starch. An Interlaboratory Comparison 79, 4603–4612. https://doi.org/10.1021/ac0700023.
Borella, S., Leuenberger, M., Saurer, M., 1999. Analysis of δ18O in tree rings: wood-cellulose comparison and method dependent sensitivity. J. Geophys. Res. Atmos. 104, 19267–19273. https://doi.org/10.1029/1999JD900298.
Bräker, O.u., 1981. Der Alterstrend bei Jahrringdichten und Jahrringbreiten von Nadelhölzern und sein Ausgleich. Mitt. Forstl. Bundesversuchsanst. Wien 142, 75–102.
Brand, W.A., Coplen, T.B., 2012. Stable isotope deltas tiny yet robust signatures in nature. Heal. Stud. 48, 393–409. https://doi.org/10.1080/10256016.2012.666977.
Briffa, K.R., Jones, P.D., Bartholin, T.S., Eckstein, D., Schweingruber, F.H., Karlén, W., Zetterberg, P., Eronen, M., 1992. Fennoscandian summers from ad 500: temperature changes on short and long timescales. Clim. Dynam. 7, 111–119. https://doi.org/10.1007/BF00211153.
Bunn, A.G., 2008. A dendrochronology program library in R (dplR). Dendrochronologia 26, 115–124. https://doi.org/10.1016/j.dendro.2008.01.002.
Büntgen, U., Kolář, T., Rybníček, M., Koňasová, E., Trnka, M., Alexander, A., Krusic, P.J., Esper, J., Treydte, K., Reinig, F., Kirdyanov, A., Herzig, F., Urban, O., 2020. No age trends in oak stable isotopes. Paleoceanogr. Paleoclimatol. 35 https://doi.org/10.1029/2019PA003831.
Büntgen, U., Urban, O., Krusic, P.J., Rybníček, M., Kolář, T., Kyncl, T., Ač, A., Koňasová, E., Čáslavský, J., Esper, J., Wagner, S., Saurer, M., Tegel, W., Dobrovolný, P., Cherubini, P., Reinig, F., Trnka, M., 2021. Recent European drought extremes beyond Common Era background variability. Nat. Geosci. 14, 190–196. https://doi.org/10.1038/s41561-021-00698-0.
Cook, E.R., Briffa, K.R., Meko, D.M., Graybill, D.A., Funkhouser, G., 1995. The 'segment length curse' in long tree-ring chronology development for palaeoclimatic studies. Holocene 5, 229–237. https://doi.org/10.1177/095968369500500211.
Daux, V., Michelot-Antalik, A., Lavergne, A., Pierre, M., Stievenard, M., Bréda, N., Damesin, C., 2018. Comparisons of the performance of δ13C and δ18O of fagus sylvatica, pinus sylvestris, and quercus petraea in the record of past climate variations. J. Geophys. Res. Biogeosciences 123, 1145–1160. https://doi.org/10.1002/2017JG004203.
Duffy, J.E., McCarroll, D., Loader, N.J., Young, G.H.F., Davies, D., Miles, D., Bronk Ramsey, C., 2019. Absence of age-related trends in stable oxygen isotope ratios from oak tree rings. Global Biogeochem. Cycles 33, 841–848. https://doi.org/10.1029/2019GB006195.
Duquesnay, A., Bréda, N., Stievenard, M., Dupouey, J.L., 1998. Changes of tree-ring δ13C and water-use efficiency of beech (Fagus sylvatica L.) in north-eastern France during the past century. Plant Cell Environ. 21, 565–572. https://doi.org/10.1046/j.1365-3040.1998.00304.x.
Dybkaer, R., 2004. Units for Quantities of Dimension One Metrologia, pp. 69–73. https://doi.org/10.1088/0026-1394/41/1/010.
Ehleringer, J.R., Field, C.B., Lin, Z., fang, Kuo, yen, C., 1986. Leaf carbon isotope and mineral composition in subtropical plants along an irradiance cline. Oecologia 70, 520–526. https://doi.org/10.1007/BF00379898.
Esper, J., Cook, E., Krusic, P., Peters, K., Schweingruber, F., 2003. Tests of the RCS method for preserving low-frequency variability in long tree-ring chronologies. Tree-Ring Res. 70, 81–98.
Esper, J., Frank, D.C., Battipaglia, G., Büntgen, U., Holert, C., Treydte, K., Siegwolf, R., Saurer, M., 2010. Low-frequency noise in δ13C and δ18O tree ring data: a case study of Pinus uncinata in the Spanish Pyrenees. Global Biogeochem. Cycles 24, 1–11. https://doi.org/10.1029/2010GB003772.
Esper, J., Frank, D.C., Wilson, R.J.S., 2004. Climate Reconstructions: Low-Frequency Ambition and High-Frequency Ratification, vol. 85. Eos, Washington. DC. https://doi.org/10.1029/2004EO120002.
Esper, J., Holzkämper, S., Büntgen, U., Schöne, B., Keppler, F., Hartl, C., George, S.S., Riechelmann, D.F.C., Treydte, K., 2018. Site-specific climatic signals in stable isotope records from Swedish pine forests. Trees Struct. Funct. 32, 855–869. https://doi.org/10.1007/s00468-018-1678-z.
Esper, J., Klippel, L., Krusic, P.J., Konter, O., Raible, C.C., Xoplaki, E., Luterbacher, J., Büntgen, U., 2020a. Eastern Mediterranean summer temperatures since 730 CE from Mt. Smolikas tree-ring densities. Clim. Dynam. 54, 1367–1382. https://doi.org/10.1007/s00382-019-05063-x.
Esper, J., Konter, O., Klippel, L., Krusic, P.J., Büntgen, U., 2021. Pre-instrumental summer precipitation variability in northwestern Greece from a high-elevation Pinus heldreichii network. Int. J. Climatol. 41, 2828–2839. https://doi.org/10.1002/joc.6992.
Esper, J., Konter, O., Krusic, P.J., Saurer, M., Holzkämper, S., Büntgen, U., 2015. Long-term summer temperature variations in the Pyrenees from detrended stable carbon isotopes. Geochronometria 42, 53–59. https://doi.org/10.1515/geochr-2015-0006.
Esper, J., Riechelmann, D.F.C., Holzkämper, S., 2020b. Circumferential and longitudinal δ13C variability in a larix decidua trunk from the swiss alps. Forests 11, 1–13. https://doi.org/10.3390/f11010117.
Francey, R.J., Farquhar, G.D., 1982. An explanation of 13C/12C variations in tree rings. Nature 297, 28–31. https://doi.org/10.1038/297028a0.
Francey, R.J., Gifford, R.M., Sharkey, T.D., Weir, B., 1985. Physiological influences on carbon isotope discrimination in huon pine (Lagarostrobos franklinii) R. J. Aust. J. Plant Physiol. 211–218.
Gagen, M., McCarroll, D., Loader, N.J., Robertson, I., Jalkanen, R., Anchukaitis, K.J., Exorcising the 'segment length curGagen, M., McCarroll, D., Loader, N.J., Robertson, I., Jalkanen, R., Anchukaitis, K.J., 2006. Exorcising the "segment length curse": summer temperature reconstruction since AD 1640 using non-detrended stable carbon isotop. Holocene 17, 435–446. https://doi.org/10.1177/0959683607077012.
Gagen, M., McCarroll, D., Robertson, I., Loader, N.J., Jalkanen, R., 2008. Do tree ring δ13C series from Pinus sylvestris in northern Fennoscandia contain long-term non-climatic trends? Chem. Geol. 252, 42–51. https://doi.org/10.1016/j.chemgeo.2008.01.013.
Gaglioti, B.V., Mann, D.H., Wooller, M.J., Jones, B.M., Wiles, G.C., Groves, P., Kunz, M. L., Baughman, C.A., Reanier, R.E., 2017. Younger-Dryas cooling and sea-ice feedbacks were prominent features of the Pleistocene-Holocene transition in Arctic Alaska. Quat. Sci. Rev. 169, 330–343. https://doi.org/10.1016/j.quascirev.2017.05.012.
Gori, Y., Wehrens, R., Greule, M., Keppler, F., Ziller, L., La Porta, N., Camin, F., 2013. Carbon, hydrogen and oxygen stable isotope ratios of whole wood, cellulose and lignin methoxyl groups of Picea abies as climate proxies. Rapid Commun. Mass Spectrom. 27, 265–275. https://doi.org/10.1002/rcm.6446.
Greule, M., Moossen, H., Geilmann, H., Brand, W.A., Keppler, F., 2019. Methyl sulfates as methoxy isotopic reference materials for δ 13 C and δ 2 H measurements. Rapid Commun. Mass Spectrom. 33, 343–350. https://doi.org/10.1002/rcm.8355.
Greule, M., Moossen, H., Lloyd, M.K., Geilmann, H., Brand, W.A., Eiler, J.M., Qi, H., Keppler, F., 2020. Three wood isotopic reference materials for δ2H and δ13C measurements of plant methoxy groups. Chem. Geol. 533, 119428 https://doi.org/10.1016/j.chemgeo.2019.119428.
Greule, M., Mosandl, A., Hamilton, J.T.G., Keppler, F., 2009. A simple rapid method to precisely determine 13C/12C ratios of plant methoxyl groups. Rapid Commun. Mass Spectrom. 23, 1710–1714. https://doi.org/10.1002/rcm.4057.
Greule, M., Mosandl, A., Hamilton, J.T.G., Keppler, F., 2008. A rapid and precise method for determination of D/H ratios of plant methoxyl groups. Rapid Commun. Mass Spectrom. 22, 3983–3988. https://doi.org/10.1002/rcm.3817.
Hafner, P., Robertson, I., McCarroll, D., Loader, N.J., Gagen, M., Bale, R.J., Jungner, H., Sonninen, E., Hilasvuori, E., Levanič, T., 2011. Climate signals in the ring widths and stable carbon, hydrogen and oxygen isotopic composition of Larix decidua growing at the forest limit in the southeastern European Alps. Trees Struct. Funct. 25, 1141–1154. https://doi.org/10.1007/s00468-011-0589-z.
Hamed, K.H., Rao, A.R., 1998. A Modified Mann-Kendall Trend Test for Autocorrelated Data 204, pp. 182–196. https://doi.org/10.1016/S0022-1694(97)00125-X.
Helama, S., Arppe, L., Timonen, M., Mielikäinen, K., Oinonen, M., 2015. Age-related trends in subfossil tree-ring δ13C data. Chem. Geol. 416, 28–35. https://doi.org/10.1016/j.chemgeo.2015.10.019.
Keeling, C.D., 1979. The Suess effect: 13Carbon-14Carbon interrelations. Environ. Int. 2, 229–300. https://doi.org/10.1016/0160-4120(79)90005-9.
Keeling, C.D., Stephen, C., Piper, S.C., Bacastow, R.B., Wahlen, M., Whorf, T.P., Heimann, M., Meijer, H.a., 2001. Exchanges of atmospheric CO2 and 13CO2 with the terrestrial biosphere and oceans from 1978 to 2000. Glob. Asp. SIO Ref. Ser. Scripps Inst. Ocean. San Diego 1 (6), 83–113.
Keeling, R.F., Graven, H.D., Welp, L.R., Resplandy, L., Bi, J., Piper, S.C., Sun, Y., Bollenbacher, A., Meijer, H.A.J., 2017. Atmospheric evidence for a global secular increase in carbon isotopic discrimination of land photosynthesis. Proc. Natl. Acad. Sci. U. S. A 114, 10361–10366. https://doi.org/10.1073/pnas.1619240114.
Keppler, F., Harper, D.B., Kalin, R.M., Meier-Augenstein, W., Farmer, N., Davis, S., Schmidt, H.L., Brown, D.M., Hamilton, J.T.G., 2007. Stable hydrogen isotope ratios of lignin methoxyl groups as a paleoclimate proxy and constraint of the geographical origin of wood. New Phytol. 176, 600–609. https://doi.org/10.1111/j.1469-8137.2007.02213.x.
Keppler, F., Kalin, R.M., Harper, D.B., McRoberts, W.C., Hamilton, J.T.G., 2004. Carbon isotope anomaly in the major plant C1 pool and its global biogeochemical implications. Biogeosciences 1, 123–131. https://doi.org/10.5194/bg-1-123-2004.
Kilroy, E., McCarroll, D., Young, G.H.F., Lo, N.J., Bale, R.J., 2016. Absence of juvenile effects confirmed in stable carbon and oxygen isotopes of european larch trees. Acta Silvae Ligni 111, 27–33. https://doi.org/10.20315/asetl.111.3.
Klippel, L., Krusic, P.J., Brandes, R., Hartl-Meier, C., Trouet, V., Meko, M., Esper, J., 2017. High-elevation inter-site differences in Mount Smolikas tree-ring width data. Dendrochronologia 44, 164–173. https://doi.org/10.1016/j.dendro.2017.05.006.
Konter, O., Esper, J., Liebhold, A., Kyncl, T., Schneider, L., Düthorn, E., Büntgen, U., 2015. Tree-ring evidence for the historical absence of cyclic larch budmoth outbreaks in the Tatra Mountains. Trees Struct. Funct. 29, 809–814. https://doi.org/10.1007/s00468-015-1160-0.
Konter, O., Holzkämper, S., Helle, G., Büntgen, U., Saurer, M., Esper, J., 2014. Climate sensitivity and parameter coherency in annually resolved δ13C and δ18O from Pinus uncinata tree-ring data in the Spanish Pyrenees. Chem. Geol. 377, 12–19. https://doi.org/10.1016/j.chemgeo.2014.03.021.
Konter, O., Krusic, P.J., Trouet, V., Esper, J., 2017. Meet Adonis, Europe's oldest dendrochronologically dated tree. Dendrochronologia 42, 12. https://doi.org/10.1016/j.dendro.2016.12.001.
Leavitt, S.W., 2010. Tree-ring C-H-O isotope variability and sampling. Sci. Total Environ. 408, 5244–5253. https://doi.org/10.1016/j.scitotenv.2010.07.057.

Lin, G., Sternberg, L., 1993. Hydrogen Isotopic Fractionation by Plant Roots during Water Uptake in Coastal Wetland Plants, Stable Isotopes and Plant Carbon-Water Relations. https://doi.org/10.1016/b978-0-08-091801-3.50041-6.

Loader, N.J., Young, G.H.F., Grudd, H., McCarroll, D., 2013. Stable carbon isotopes from Torneträsk, northern Sweden provide a millennial length reconstruction of summer sunshine and its relationship to Arctic circulation. Quat. Sci. Rev. 62, 97–113. https://doi.org/10.1016/j.quascirev.2012.11.014.

Lu, Q., Liu, X., Tan, L., Keppler, F., Treydte, K., Wieland, A., Zhang, L., Shi, X., Zhang, Y., Wang, Y., Zeng, X., Liu, J., Zhao, L., Xu, G., Xing, X., 2022. Tree-ring δ2H records of lignin methoxy indicate spring temperature changes since 20th century in the Qinling Mountains, China. Dendrochronologia 76, 126020. https://doi.org/10.1016/j.dendro.2022.126020.

Lukač, L., Mikac, S., Urban, O., Kolář, T., Rybníček, M., Ač, A., Trnka, M., Marek, M.V., 2021. Stable isotopes in tree rings of pinus heldreichii can indicate climate variability over the eastern mediterranean region. Forests 12, 1–14. https://doi.org/10.3390/f12030350.

McCarroll, D., Jalkanen, R., Hicks, S., Tuovinen, M., Gagen, M., Pawellek, F., Eckstein, D., Schmitt, U., Autio, J., Heikkinen, O., 2003. Multiproxy dendroclimatology: a pilot study in northern Finland. Holocene 13, 829–838. https://doi.org/10.1191/0959683603hl668rp.

McCarroll, D., Loader, N.J., 2004. Stable isotopes in tree rings. Quat. Sci. Rev. 23, 771–801. https://doi.org/10.1016/j.quascirev.2003.06.017.

McCarroll, D., Pawellek, F., 2001. Stable carbon isotope ratios of Pinus sylvestris from northern Finland and the potential for extracting a climate signal from long Fennoscandian chronologies. Holocene 11, 517–526. https://doi.org/10.1191/095968301680223477.

McDowell, N.G., Phillips, N., Lunch, C., Bond, B.J., Ryan, M.G., 2002. An investigation of hydraulic limitation and compensation in large, old Douglas-fir trees. Tree Physiol. 22, 763–774. https://doi.org/10.1093/treephys/22.11.763.

Melvin, T.M., Briffa, K.R., 2014. CRUST: software for the implementation of regional chronology standardisation: Part 1. Signal-free RCS. Dendrochronologia 32, 7–20. https://doi.org/10.1016/j.dendro.2013.06.002.

Melvin, T.M., Briffa, K.R., 2008. A "signal-free" approach to dendroclimatic standardisation. Dendrochronologia 26, 71–86. https://doi.org/10.1016/j.dendro.2007.12.001.

Mischel, M., Esper, J., Keppler, F., Greule, M., Werner, W., 2015. δ2H, δ13C and δ18O from whole wood, α-cellulose and lignin methoxyl groups in Pinus sylvestris: a multi-parameter approach. Isot. Environ. Health Stud. 51, 553–568. https://doi.org/10.1080/10256016.2015.1056181.

Nakatsuka, T., Sano, M., Li, Z., Xu, C., Tsushima, A., Shigeoka, Y., Sho, K., Ohnishi, K., Sakamoto, M., Ozaki, H., Higami, N., Nakao, N., Yokoyama, M., Mitsutani, T., 2020. A 2600-year summer climate reconstruction in central Japan by integrating tree-ring stable oxygen and hydrogen isotopes. Clim. Past 16, 2153–2172. https://doi.org/10.5194/cp-16-2153-2020.

Newell, D.B., Tiesinga, E., 2019. The International System of Units (SI), vol. 330. NIST Spec. Publ. https://doi.org/10.6028/NIST.SP.330-2019.

Raffalli-Delerce, G., Masson-Delmotte, V., Dupouey, J.L., Stievenard, M., Breda, N., Moisselin, J.M., 2004. Reconstruction of summer droughts using tree-ring cellulose isotopes: a calibration study with living oaks from Brittany (western France). Tellus Ser. B Chem. Phys. Meteorol. 56, 160–174. https://doi.org/10.1111/j.1600-0889.2004.00086.x.

Riechelmann, D.F.C., Greule, M., Siegwolf, R.T.W., Anhäuser, T., Esper, J., Keppler, F., 2017. Warm season precipitation signal in δ2H values of wood lignin methoxyl groups from high elevation larch trees in Switzerland. Rapid Commun. Mass Spectrom. 31, 1589–1598. https://doi.org/10.1002/rcm.7938.

Römer, P., Reinig, F., Konter, O., Friedrich, R., Urban, O., Čáslavský, J., Pernicová, N., Trnka, M., Büntgen, U., Esper, J., 2023. Multi-proxy crossdating extends the longest high-elevation tree-ring chronology from the Mediterranean. Dendrochronologia 79. https://doi.org/10.1016/j.dendro.2023.126085.

Stokes, M.A., Smiley, T.L., 1996. An Introduction to Tree-Ring Dating. The University of Arizona Press.

Torbenson, M., Klippel, L., Hartl, C., Reinig, F., Treydte, K., Büntgen, U., Trnka, M., Schöne, B., Schneider, L., Esper, J., 2022. Investigation of age trends in tree-ring stable carbon and oxygen isotopes from northern Fennoscandia over the past millennium. Quat. Int. https://doi.org/10.1016/j.quaint.2022.05.017.

Treydte, K., Schleser, G., Schweingruber, F., Winiger, M., 2001. The climatic significance of δ 13 C in subalpine spruces (Lötschental, Swiss Alps) : a case study with respect to altitude, exposure and soil moisture. Tellus B 53, 593–611. https://doi.org/10.3402/tellusb.v53i5.16639.

Treydte, K.S., Schleser, G.H., Helle, G., Frank, D.C., Winiger, M., Haug, G.H., Esper, J., 2006. The twentieth century was the wettest period in northern Pakistan over the past millennium. Nature 440, 1179–1182. https://doi.org/10.1038/nature04743.

Urey, H.C., 1948. Oxygen isotopes in nature and in the laboratory. Science (80- 108, 489–496. http://www.jstor.org/stable/1677444.

van der Merwe, N.J., Medina, E., 1991. The canopy effect , carbon isotope ratios and foodwebs in amazonia. J. Archaeol. Sci. 18, 249–259. https://doi.org/10.1016/0305-4403(91)90064-V.

Vogel, J., 1978. Recycling of carbon in a forest environment. Oecol. Plant. 13, 89–94.

Wieland, A., Greule, M., Roemer, P., Esper, J., Keppler, F., 2022. Climate signals in stable carbon and hydrogen isotopes of lignin methoxy groups from southern German beech trees. Clim. Past 18, 1849–1866. https://doi.org/10.5194/cp-18-1849-2022.

Zeisel, S., 1885. Über ein Verfahren zum quantitativen Nachweise von Methoxyl. Monatsh. Chem. 989–997. https://doi.org/10.1007/BF01554683.